Research Article

INTERNATIONAL JOURNAL OF ADVANCED ROBOTIC SYSTEMS

International Journal of Advanced Robotic Systems
January-February 2018: 1–10

DOI: 10.1177/1729881417749483
journals.sagepub.com/home/arx
SAGE

Backstepping control based on L_1 adaptive theory for large transport aircraft heavy load airdrop

Pengchao Zhang

Abstract

A study of the L_1 adaptive controller is conducted based on the backstepping method for the model of large transport aircraft with drastic changes appearing in heavy load airdrop process. The system is divided into an attitude subsystem and a velocity subsystem. For the attitude subsystem, the backstepping control is used to design the virtual control of path angle and the pitch angle in external loop with the L_1 adaptive controller designed in internal loop to estimate the uncertainties and disturbances in the subsystem and to compensate them. In the stability analysis, the uniform boundedness of all signals in the closed-loop system is proven. Simulation results show that the proposed control method preserves the quick dynamic torque response, high efficiency, and robustness in heavy load airdrop; to some extent it can alleviate the control switch lead or lag problem and ensure the safety of the transport aircraft to fulfill the complete airdrop mission.

Keywords

Heavy load airdrop, backstepping, L_1 adaptive control, uncertainties, virtual control

Date received: 25 July 2017; accepted: 29 October 2017

Topic: Special Issue—Modeling and Control during Airdrop Process
Topic Editor: Yangquan Chen
Associate Editor: Bin Xu

Introduction

Large air transport and precision airdrop plays an important role in military and rescue operation, with the airdrop ability being an important indicator of national defense force and the significant means for rapid response and long distance maneuvers in a modern war.

However, the robust and precise airdrop is difficult to carry out due to model mutation occurring especially during the large transport heavy drop. The aircraft controller cannot be switched accurately during airdrop, that is to say, the switch can occur either ahead or lagged, causing intense oscillation or machine apart. This problem belongs to the mutation model control,[1–3] and it is necessary to solve it properly for the safety of large transport aircrafts.

Currently, the study of transport load airdrop focuses on the analysis,[4,5] modeling,[6] simulation,[7,8] and control law design.[6,9] In the study by Jann,[8] the general military airdrop process of longitudinal channel is simulated, with the influence of airdrop on the flight control system studied by Chen et al.[6,9] At the moment of cargo separating from aircraft, the large angle of attack motion and the problem from controlling models of security are shown in the literatures.[10–13] The variable structure control in Xu and Sun[14] and sliding mode control in Zhang and Shi[15] are also studied to ensure the safety of the aircraft.

With the development of the modern control theory, many methods[16–21] are useful in improving the robustness of the system. In earlier works,[17,20] the discrete adaptive

Shaanxi Provincial Key Laboratory of Industrial Automation, Shaanxi University of Technology, Shaanxi, Hanzhong, China

Corresponding author:
Pengchao Zhang, Shaanxi Provincial Key Laboratory of Industrial Automation, Shaanxi University of Technology, Shaanxi, Hanzhong 723000, China
Email: snutzpc@126.com

backstepping is studied for a class of uncertain systems and they are also applied in helicopter control by Li et al.[22] To deal with the calculation explosion, the dynamic surface control and instruction filter are introduced in the study by Xu.[23] The backstepping combined with sliding control is introduced in the longitudinal sliding mode adaptive controller for the unmatched and uncertain longitudinal parameters. The L_1 adaptive control theory is presented by Cao and Hovakimyan[24,25] and widely used later. Compared to the conventional adaptive control, L_1 adaptive control can make the regulation time shorter and ensure better asymptotic tracking and transient performance in the delay system.[26–29]

For the instability of control system by model mutation during the ultra low altitude airdrop, this article presents a method combined with backstepping and the L_1 adaptive method for obtaining the robust and precision airdrop. The backstepping method is used for the controller of track angle and pitching angle in the attitude subsystem. The L_1 adaptive controller is carried on the estimation and compensation to improve the dynamic performance and robustness. Through the design of virtual control, compensation is made to solve the problem of calculation explosion, ensuring the stability and reliability. Simulation results show the effectiveness and strong robustness of the method proposed in this article.

The article structure is as follows. The airdrop model is presented in the dynamic model section, the design of controller is given in the third section, an analysis of stability is made in the fourth section, in fifth section, simulation results show the effectiveness of the control method, and the conclusion is drawn in the last section.

Dynamic model

In this article, the force in the airdrop process of the aircraft is analyzed and for the cargo movement displacement as additional state variables, the dynamic model from Christopher et al.[26] can be described as follows

$$\begin{aligned}
\dot{V} &= \frac{\left(T + F_b - m_b(\ddot{d} - dq^2)\right)\cos\alpha + m_b(2\dot{d}q + d\dot{q})\sin\alpha}{m} \\
&\quad - \frac{W}{m} - g\sin\gamma \\
\dot{\alpha} &= \frac{m_b(2\dot{d}q + d\dot{q})\cos\alpha - A - (T + F_b - m_b(\ddot{d} - dq^2))\sin\alpha}{mV} \\
&\quad + \frac{g\cos\gamma}{V} + q \\
\dot{\theta} &= q \\
\dot{q} &= \frac{M}{I_y} \\
\dot{H} &= V\sin\gamma \\
\ddot{d} &= dq^2 + \mu(2\dot{d}q + d\dot{q}) + \frac{F_b}{m_b} \\
&\quad + \frac{\left(A(-\sin\alpha + \mu\cos\alpha) + W(\cos\alpha + \mu\sin\alpha)c_\alpha + T\right)}{m_a}
\end{aligned} \tag{1}$$

Table 1. Miscellaneous coefficient values.

Coefficient	Value	Units
S	5.500×10^3	$ft^2 \cdot ft^{-1}$
ρ	1.225×10^0	$slugs \cdot ft^{-3}$
I_{yy}	3.050×10^7	$lb \cdot ft$
m_a	1.753×10^4	$lb \cdot ft^{-1}$
g	3.200×10^1	$ft \cdot s^{-2}$
I_{yyb}	2.3627×10^5	$lb \cdot ft$
m_b	2.6038×10^3	$lb \cdot ft^{-1}$
α_0	0.0349×10^0	rad
μ	0.01×10^0	—
k_u	0.1655×10^0	—

Table 2. Lift coefficient values.

Coefficient	Value	Units
C_{A0}	2.030×10^0	—
$C_{A\alpha}$	8.000×10^0	rad^{-1}
$C_{A\dot{\alpha}}$	6.700×10^0	$rad^{-1} \cdot s$
C_{AV}	0.220×10^0	$ft^{-1} \cdot s$
C_{Aq}	5.650×10^0	$rad^{-1} \cdot s$
$C_{A\delta_e}$	1.110×10^0	rad^{-1}

In equation (1), V is the plane velocity; α is the attack angle; θ is the pitch angle; H is the altitude; q is the pitch rate; d is the distance of the first cargo moved away; γ is *the* flight path angle and $\gamma = \theta - \alpha$; F_b is the traction for cargos movement and $F_b = -k_u m_b g$; m is the sum of the mass of aircraft and cargos and $m = m_a + m_b$, where m_a is the aircraft mass and m_b is the cargo mass; T is the push force and $T = T_{\max}\delta_T$, where $T_{\max}$ is the maximum of the push force and δ_T is fuel equivalence ratio; A is the lift force and $A = C_A QS$; W is the drag force and $W = C_W QS$; Q is the kinetic pressure and $Q = \frac{1}{2}\rho V^2$;S is the wing area; C_A is the coefficient to lift; C_W is the coefficient to drag, and

$$\begin{aligned}
C_A &= C_{A0} + C_{A\alpha}(\alpha - \alpha_0) + C_{A\dot{\alpha}}\frac{\dot{\alpha}c_A}{2V} + C_{Aq}\frac{qc_A}{2V} \\
&\quad + C_{AV}(V - V_0) + C_{A\delta_e}\delta_e \\
C_W &= C_{W0} + C_{W\alpha}(\alpha - \alpha_0) + C_{WV}(V - V_0) + C_{W\delta_e}\delta_e
\end{aligned}$$

In the dynamic model, $M = M_A + M_B + M_T$, M_A is the pitch moment, M_B is the additional moment caused by the moving cargo, and M_T is the thrust moment. They are expressed as

$$\begin{aligned}
M_A &= QSc_A[C_{M0} + C_{M\alpha}(\alpha - \alpha_0) + C_{mV}(V - V_0) \\
&\quad + C_{M\dot{\alpha}}\frac{\dot{\alpha}c_A}{2V} + C_{Mq}\frac{qc_A}{2V} + C_{M\delta_e}\delta_e] \\
M_B &= -nd(A\cos\alpha + W\sin\alpha) \\
M_T &= z_p T
\end{aligned} \tag{2}$$

where n is the ratio of m_b and m, I_y is the total inertia of plane and the rest load. The values and units are listed in Tables 1 to 5.

Table 3. Drag coefficient values.

Coefficient	Value	Units
C_{W0}	0.263×10^{0}	–
$C_{W\alpha}$	1.130×10^{0}	rad^{-1}
C_{WV}	0	$ft^{-1} \cdot s$
$C_{W\delta_e}$	0	rad^{-1}

Table 4. Moment coefficient values.

Coefficient	Value	Units
z_T	0	ft
c_A	2.730×10^{1}	ft
C_{M0}	1.8979×10^{-1}	–
$C_{M\alpha}$	-1.450×10^{0}	rad^{-1}
$C_{M\dot{\alpha}}$	-3.300×10^{0}	$rad^{-1} \cdot s$
C_{MV}	0.071×10^{0}	$ft^{-1} \cdot s$
C_{Mq}	-2.140×10^{1}	$rad^{-1} \cdot s$
$C_{M\delta_e}$	-4.400×10^{0}	rad^{-1}

Remark 1. When all the cargos are dropped, the system model from Christopher et al.[26] is

$$\begin{aligned}
\dot{V} &= \frac{T\cos\alpha - W}{m} - g\sin\gamma \\
\dot{\alpha} &= -\frac{T\sin\alpha + A}{mV} + \frac{g\cos\gamma}{V} + q \\
\dot{\theta} &= q \\
\dot{q} &= \frac{M}{I_y} \\
\dot{H} &= V\sin\gamma
\end{aligned} \tag{3}$$

Controller design

As the track angle γ is little, it is assumed that $\sin\gamma = \gamma$. In the $H - \gamma$ subsystem, the track error is defined as $\tilde{H} = H - H_r$, and then the instruction for the track angle can be calculated as

$$\gamma_d = \arcsin\left[\frac{-k_P(H - H_r) - k_I\int(H - H_r)dt + k_D\dot{H}_r}{V}\right] \tag{4}$$

where the PID parameters k_P, k_I, and k_D can be set by the designer.

When the track angle approaches the expected γ_d, a height index tracking error converges to zero. Through the instruction transformation, the height control can be achieved through the attitude control.

Define the state variables $x = [\gamma \quad \theta \quad q]^T$. The dynamic equations of attitude subsystem can be written as

Table 5. Thrust coefficient values.

Coefficient	Value	Units
T_{max}	2.190×10^{5}	$lb \cdot s^{-2}$

$$\begin{cases}
\dot{x}_1 = f_1 + g_1 x_2 \\
\dot{x}_2 = f_2 + g_2 x_3 \\
\dot{x}_3 = f_3 + g_3 u \\
y = x \\
u = \delta_e
\end{cases} \tag{5}$$

Velocity subsystem can be written in the following form

$$\begin{cases}
\dot{V} = f_V + g_V u_V \\
y = V \\
u_V = \delta_T
\end{cases}$$

where $f_1 = -\dfrac{m_b(2\dot{d}q + d\dot{q})\cos\alpha - (A - C_{A\alpha}\theta QS)}{mV} - \dfrac{\left(T + F_b - F_b - m_b(\ddot{d} - dq^2)\right)\sin\alpha}{mV} - \dfrac{g\cos\gamma}{V}$, $g_1 = \frac{C_{A\alpha}QS}{mV}$, $f_2 = 0$, $g_2 = 1$, $f_3 = \frac{M}{I_y} - \frac{C_{M\delta_e}\delta_e QSc_A}{I_y}$, $g_3 = \frac{C_{M\delta_e}QSc_A}{I_y}$, $f_V = \dfrac{(F_b - m_b(\ddot{d} - dq^2))\cos\alpha + m_b(2\dot{d}q + d\dot{q})\sin\alpha}{m} - \dfrac{W}{m} - g\sin\gamma$, $g_V = \dfrac{T_{max}\cos\alpha}{m}$

Attitude subsystem model

The attitude subsystem was composed of track angle parts, pitching angle parts, and pitching angle rate parts. It was divided into the external loop and internal loop subsystems.

The external loop subsystem is as follows

$$\begin{cases}
\dot{x}_1 = f_1 + g_1 x_2 \\
\dot{x}_2 = f_2 + g_2 x_3
\end{cases}$$

The internal loop subsystem is

$$\dot{x}_3 = f_3 + g_3 u$$

By introducing the dynamic surface control to the external loop and L_1 adaptive control to the internal loop, the controller diagram is shown in Figure 1.

According to the track angle instruction γ_d , the repeated virtual control is used to achieve the control effect with instruction filter introduced to solve the traditional problems of "calculation explosion." The x_{3x} is the input variable in L_1 adaptive controller and the control law u can be obtained to control the height by tracking γ_d.

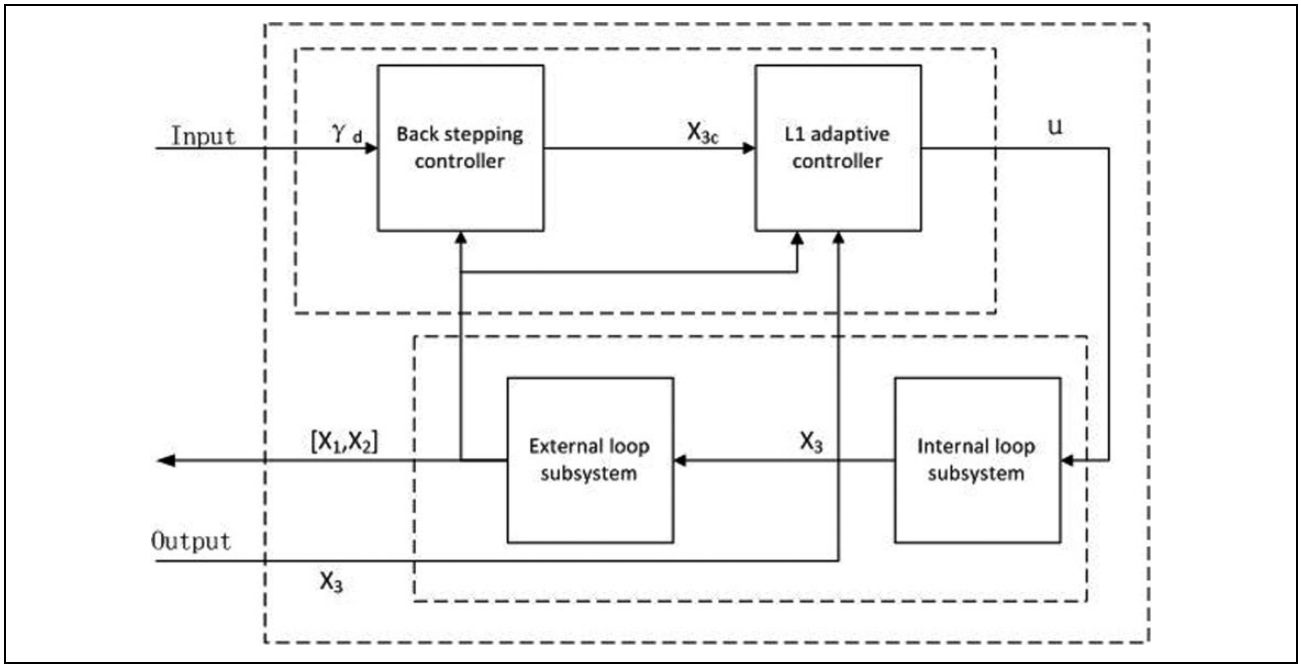

Figure 1. Attitude subsystem control diagram.

Backstepping control

Step 1. According to the equation $\dot{x}_1 = f_1 + g_1 x_2$, $e_1 = x_1 - x_{1d}$ is defined, with the tracking error of track angle being

$$\dot{e}_1 = f_1 + g_1 x_2 - \dot{x}_{1d} \tag{6}$$

x_{2c} is chosen as a virtual variable, and its design value is

$$x_{2c} = [-k_1 e_1 + \dot{x}_{1d} - f_1]/g_1 \tag{7}$$

where k_1 is a positive design parameter.

There is the new signal x_{2d} and $\dot{x}_{2d}$ which follow

$$\varepsilon_2 \dot{x}_{2d} + x_{2d} = x_{2c} \tag{8}$$

where $x_{2d}(0) = x_{2c}(0)$.

Define $y_2 = x_{2d} - x_{2c}$, $e_2 = x_2 - x_{2d}$, equation (6) can be written as

$$\dot{e}_1 = g_1(e_2 + y_2) - \dot{x}_{1d} \tag{9}$$

Step 2. The definition of $e_2 = x_2 - x_{2d}$ is similar to that in step 1. The dynamic equation of pitching angle error e_2 is $\dot{e}_2 = f_2 + g_2 x_3 - \dot{x}_{2d}$.

Define x_{3c} as virtual parameter, there is

$$x_{3c} = [-k_2 e_2 + \dot{x}_{2d} - f_2 - g_1 e_1]/g_2 \tag{10}$$

where k_2 is a positive design parameter. Equation (8) can be written as

$$\dot{e}_1 = k_2 e_2 - g_1 e_1 \tag{11}$$

L_1 adaptive controller. The internal loop subsystem $\dot{x}_3 = f_3 + g_3 u$ can be described in the linear time-varying system as

$$\begin{cases} \dot{x}_3 = Ax_3 + B(u + \rho x_3 + \sigma) \\ y = cx_3 \end{cases} \tag{12}$$

where $A = 0$, $B = g_3$, $c = 1$, and $u = \delta_e$ is the control signal, with ρ and σ being the estimated time-varying parameters. Some assumptions are needed for the convenience of controller design.

Assumption 1. Unknown parameters ρ and σ are uniformly bounded. For known tight convex set Θ and Δ, there is $\rho(t) \in \Theta$, $\sigma(t) \in \Delta$, $\forall t \geq 0$.

Assumption 2. Unknown parameters ρ and σ are continuous, differentiable, and uniformly bounded. There is $|\dot{\rho}(t)| \leq d_\rho < \infty$ and $|\dot{\sigma}(t)| \leq d_\sigma < \infty$ for $\forall t \geq 0$, where d_ρ and d_σ are constant.

L_1 control law is composed of two parts

$$u = u_1 + u_2 \tag{13}$$

where $u_1 = -Kx_3$ is the static feedback part, K is the state feedback gain, and u_2 is adaptive control part to compensate the uncertainty. The internal loop subsystem can be described by

$$\dot{x}_3 = A_o x_3 + Bb\,(u_2 + \rho x_3 + \sigma) \tag{14}$$

As the introduced state feedback control, the transfer function is as follows

$$H_o(s) = (sI - A_o)^{-1} B \tag{15}$$

In this article, the used state prediction model is

$$\dot{\hat{x}}_3 = A_o \hat{x}_3 + b(u_2 + \hat{\rho} x_3 + \hat{\sigma}) \tag{16}$$

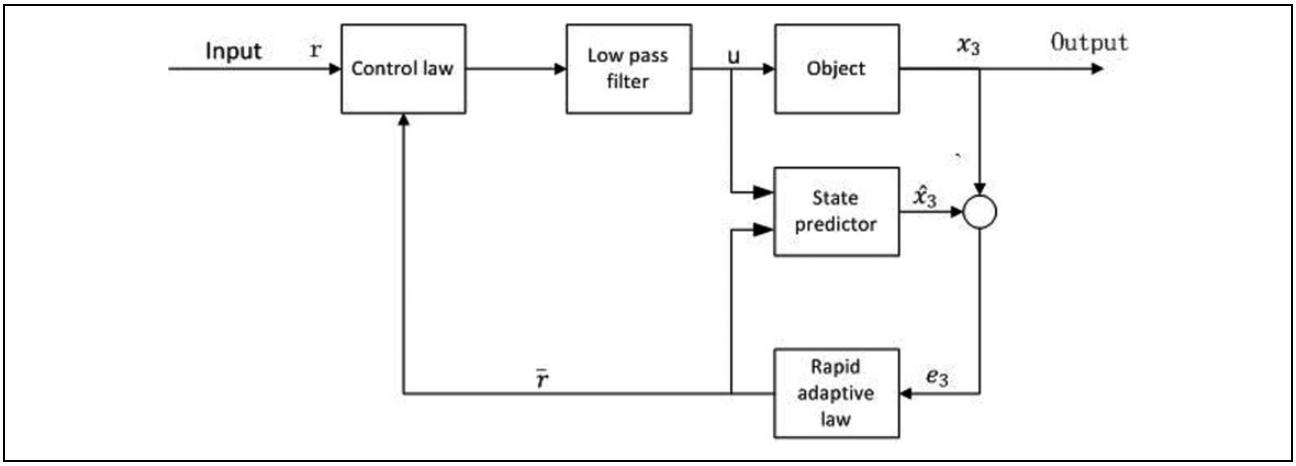

Figure 2. L_1 adaptive controller diagram.

Define the state prediction error $e_3 = \hat{x}_3 - x_3$, there is

$$\dot{e}_3 = \dot{\hat{x}}_3 - \dot{x}_3 = A_o e_3 + b(\tilde{\rho} x_3 + \tilde{\sigma}) \tag{17}$$

L_1 adaptive update law is in the following

$$\dot{\hat{\rho}} = \Gamma \, \mathrm{Pro}j(\hat{\rho}, -x_3 e_3 P b), \ \hat{\rho}(0) = \hat{\rho}_0 \tag{18}$$

$$\dot{\hat{\sigma}} = \Gamma \, \mathrm{Pro}j(\hat{\sigma}, -e_3 P b), \ \hat{\sigma}(0) = \hat{\sigma}_0 \tag{19}$$

Estimate errors are $\tilde{\rho} = \hat{\rho} - \rho$, $\tilde{\sigma} = \hat{\sigma} - \sigma$ and the dynamic equation is

$$\begin{cases} \dot{\tilde{\rho}} = \dot{\hat{\rho}} - \dot{\rho} = \Gamma \, \mathrm{Pro}j\,(\hat{\rho}, -x_3 e_3 P b) - \dot{\rho} \\ \dot{\tilde{\sigma}} = \dot{\hat{\sigma}} - \dot{\sigma} = \Gamma \, \mathrm{Pro}j\,(\hat{\sigma}, -e_3 P b) - \dot{\sigma} \end{cases}$$

where $\Gamma > 0$ and $P > 0$ is the solution of Lyapunov equation ${A_o}^T P + P A_o = 2 P A_o = -Q$.

Then the adaptive controller can be designed as

$$u_2(s) = C(s)\Big(\bar{r}(s) + k_g r(s)\Big) \tag{20}$$

where $u_2(s)$, $\bar{r}(s)$, and $r(s)$ are the Laplace of $u_2(t)$, $\bar{r}(t)$, $r(t)$, and $\bar{r}(t) = -\Big(\hat{\rho}^T(t) x(t) + \hat{\sigma}(t)\Big)$.

So, the L_1 controller diagram is shown in Figure 2 .

In all, the prediction model of loop system is in the following

$$\begin{aligned} \dot{\hat{x}}(s) &= \bar{G}(s)\bar{r}(s) + G(s) r(s) \\ \bar{G}(s) &= H_o(s)\Big(C(s) - 1\Big) \\ G(s) &= k_g H_o(s) C(s) \end{aligned} \tag{21}$$

It is necessary for the L_1 adaptive controller to satisfy the following conditions

$$\lambda = ||H_o(s)\Big(C(s) - 1\Big)||_{L_1} \rho_{\max} < 1 \tag{22}$$

where $\rho_{\max} = \max\limits_{\theta \in \Omega} \sum\limits_{i=1}^{n} |\rho_i|$.

Velocity subsystem controller

According to $\dot{V} = f_V + g_V \delta_T$, the velocity track error is defined as $e_V = V - V_r$, with its dynamic error equation

$$\dot{e}_V = f_V + g_V \delta_T - \dot{V}_r \tag{23}$$

The expected controller is

$$\delta_{Tc} = [-k_V e_V - f_V]/g_V \tag{24}$$

where k_V is the designed parameter and $k_V > 0$.

So, equation (23) can be written as

$$\dot{e}_V = -k_V e_V \tag{25}$$

Stability analysis

Proof 1. Select the Lyapunov function for the external loop subsystem in the following

$$L_1 = \frac{1}{2} e_1^2 + \frac{1}{2} y_2^2 \tag{26}$$

$$L_2 = \frac{1}{2} e_2^2 \tag{27}$$

Taking the derivative of $L_i (i = 1, 2)$, the following equations can be obtained

$$\begin{aligned} \dot{L}_1 &= e_1 \dot{e}_1 + y_2 \dot{y}_2 \\ &= -k_1 e_1^2 + g_1 (e_2 + y_2) e_1 + y_2 \left(-\frac{y_2}{\varepsilon_2} + M_2 \right) \end{aligned} \tag{28}$$

$$\dot{L}_2 = e_2 \dot{e}_2 = -k_2 e_2^2 - g_1 e_1 e_2 \tag{29}$$

$$\dot{L}_1 + \dot{L}_2 = -k_1 e_1^2 + g_1 e_1 y_2 - \frac{y_2^2}{\varepsilon_2} + y_2 M_2 - k_2 e_2^2 \quad (30)$$

As
$e_1 y_2 \le \frac{1}{2} e_1^2 + y_2^2$ and $y_2 M_2 \le \frac{1}{2} y_2^2 + \frac{1}{2} M_2^2$, formula (30) can be rewritten as

$$\begin{aligned} \dot{L}_1 + \dot{L}_2 \le & -\left(k_1 - \frac{g_1}{2}\right) e_1^2 - \left(\frac{1}{\varepsilon_2} - \frac{1}{2} - \frac{g_1}{2}\right) y_2^2 \\ & - \left(k_2 - \frac{g_2}{2}\right) e_2^2 + \frac{1}{2} M_2^2 \end{aligned} \quad (31)$$

For
$k_{10} = k_1 - \frac{g_1}{2} > 0$, $\frac{1}{\varepsilon_2} - \frac{1}{2} - \frac{g_1}{2} > 0$, $k_{20} = k_2 - \frac{g_2}{2} > 0$, the following equation can be obtained

$$\dot{L}_1 + \dot{L}_2 \le -k_{10} e_1^2 - k_{20} e_2^2 + C \quad (32)$$

$$|e_i| \le \sqrt{C/k_{i0}} \quad (33)$$

The dynamic errors e_1 and e_2 are all bounded, so the external loop subsystem is stable.

Select the Lyapunov function of the internal loop subsystem in the following

$$L_3 = P e_3^2 + \frac{1}{\Gamma} \tilde{\rho}^2 + \frac{1}{\Gamma} \tilde{\sigma}^2 \quad (34)$$

Taking the derivative of (34), there is

$$\begin{aligned} \dot{L}_3 &= 2P e_3 \dot{e}_3 + \frac{2}{\Gamma} \tilde{\rho} \dot{\tilde{\rho}} + \frac{2}{\Gamma} \tilde{\sigma} \dot{\tilde{\sigma}} \\ &= 2PA_o e_3^2 + 2Pb(\tilde{\rho} x_3 e_3 + \tilde{\sigma} e_3) + \frac{2}{\Gamma} \tilde{\rho}(\dot{\tilde{\rho}} - \dot{\rho}) \\ &\quad + \frac{2}{\Gamma} \tilde{\sigma}(\dot{\tilde{\sigma}} - \dot{\sigma}) \\ &\le -Q e_3^2 - \frac{2}{\Gamma} \tilde{\rho} \dot{\rho} - \frac{2}{\Gamma} \tilde{\sigma} \dot{\sigma} \\ &\le -Q e_3^2 + \frac{2}{\Gamma} |\tilde{\rho} \dot{\rho} + \tilde{\sigma} \dot{\sigma}| \end{aligned} \quad (35)$$

$$L = L_1 + L_2 + L_3 \quad (36)$$

The projection operator guarantees that $\rho \in \Phi$ and $\sigma \in \Delta$, and therefore the following formula is established

$$\max_{t \ge 0} \left(\tilde{\rho}^2 + \tilde{\sigma}^2\right) \le 4\left(\max_{\rho \in \Theta} \rho^2 + \max_{\sigma \in \Delta} \sigma^2\right) \quad (37)$$

Suppose $L_3 \ge \rho_m / \Gamma$, where

$$\begin{aligned} \rho_m = & \frac{4P}{Q}\left(d_\rho \max_{\rho \in \Theta} |\rho| + d_\sigma \max_{\sigma \in \Delta} |\sigma|\right) \\ & + 4\left(\max_{\rho \in \Theta} \rho^2 + \max_{\sigma \in \Delta} \sigma^2\right) \end{aligned} \quad (38)$$

Table 6. Different trim conditions for airdrop.

V(ft · s^{-1})	H(ft)	$\alpha(^\circ)$	$\theta(^\circ)$	$\delta_e(^\circ)$
221	16.404	1.9376	1.9376	0.0229
200	16.404	5.1535	5.1535	−1.0376
221	24.606	1.9433	1.9433	0.0172
200	24.606	5.1592	5.1592	−1.0376

$$\begin{aligned} L_3 &= P e_3^2 + \frac{1}{\Gamma} \tilde{\rho}^2 + \frac{1}{\Gamma} \tilde{\sigma}^2 \\ &\ge \frac{4P}{Q\Gamma}\left(d_\rho \max_{\rho \in \Theta} |\rho| + d_\sigma \max_{\sigma \in \Delta} |\sigma|\right) \\ &\quad + \frac{4}{\Gamma}\left(\max_{\rho \in \Theta} \rho^2 + \max_{\sigma \in \Delta} \sigma^2\right) \end{aligned} \quad (39)$$

then equation (40) is obtained

$$P e_3^2 \ge \frac{4P}{Q\Gamma}\left(d_\rho \max_{\rho \in \Theta} |\rho| + d_\sigma \max_{\sigma \in \Delta} |\sigma|\right) \quad (40)$$

For $P > 0$, there is

$$Q e_3^2 \ge \frac{4}{\Gamma}\left(d_\rho \max_{\rho \in \Theta} |\rho| + d_\sigma \max_{\sigma \in \Delta} |\sigma|\right) \quad (41)$$

From assumptions 1 and 2, the following equation can be obtained

$$|\tilde{\rho} \dot{\rho} + \tilde{\sigma} \dot{\sigma}| \le 2\left(d_\rho \max_{\rho \in \Theta} |\rho| + d_\sigma \max_{\sigma \in \Delta} |\sigma|\right) \quad (42)$$

Putting (41) and (42) into (35), there is

$$\dot{L}_3 \le 0 \quad (43)$$

Suppose that $|e_1(0)| + |e_2(0)| \le d_c < \infty$, that d_c is bounded constant, that $y_2(0) = x_{2d}(0) - x_{2c}(0) = 0$, and that $e_3(0) = 0$, which yields

$$\begin{aligned} L(0) &= L_1(0) + L_2(0) + L_3(0) \\ &= \frac{1}{2} e_1^2(0) + \frac{1}{2} y_2^2(0) + \frac{1}{2} e_2^2(0) + P e_3^2(0) + \frac{1}{\Gamma} \tilde{\rho}^2 + \frac{1}{\Gamma} \tilde{\sigma}^2 \\ &\le \frac{1}{2} d_c^2 + \frac{4}{\Gamma}\left(\max_{\rho \in \Theta} \rho^2 + \max_{\sigma \in \Delta} \sigma^2\right) \\ &\le \frac{1}{2} d_c^2 + \frac{\rho_m}{\Gamma} \end{aligned}$$

Thus

$$L(t) \le L(0) \le \frac{1}{2} d_c^2 + \frac{4}{\Gamma}\left(\max_{\rho \in \Theta} \rho^2 + \max_{\sigma \in \Delta} \sigma^2\right) \quad (44)$$

So the attitude subsystem is stable.

Proof 2. Select the following Lyapunov function

$$L_V = \frac{1}{2} e_V^2 \quad (45)$$

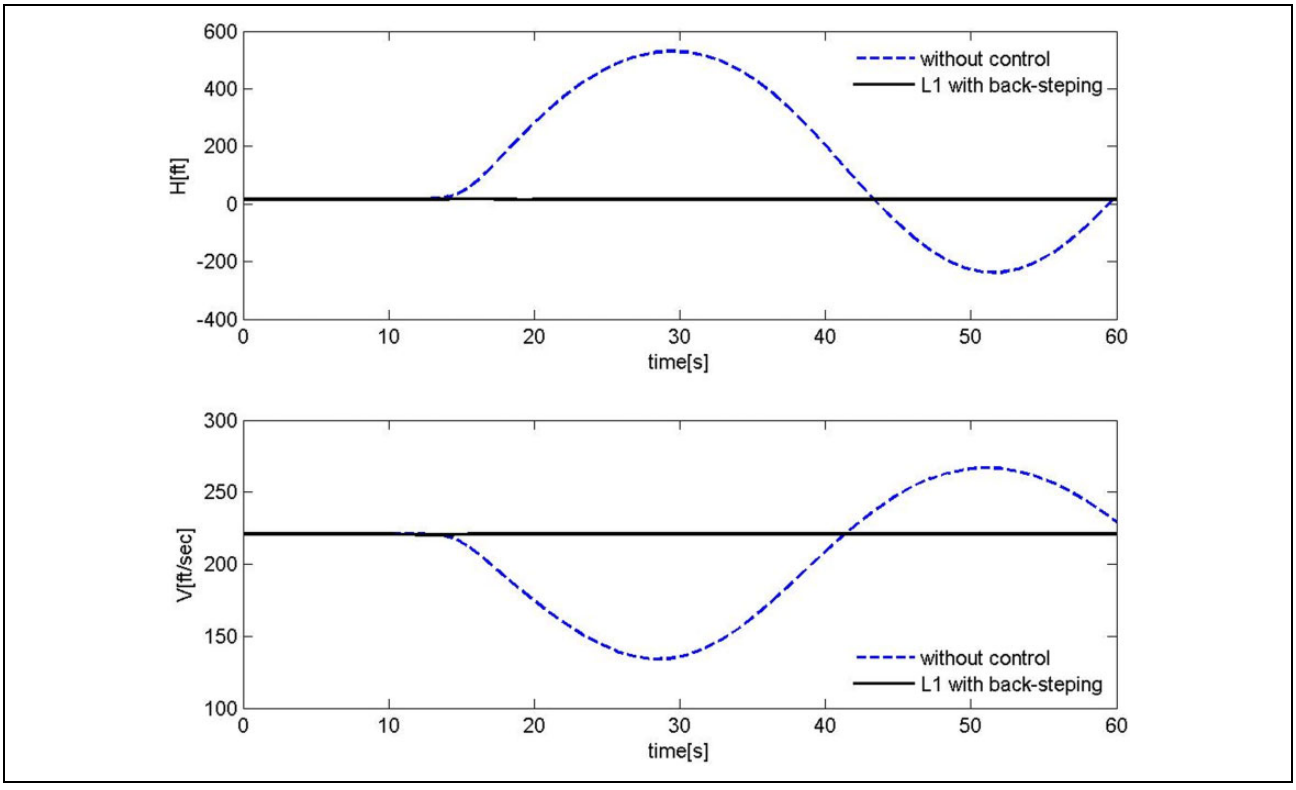

Figure 3. Altitude and velocity response.

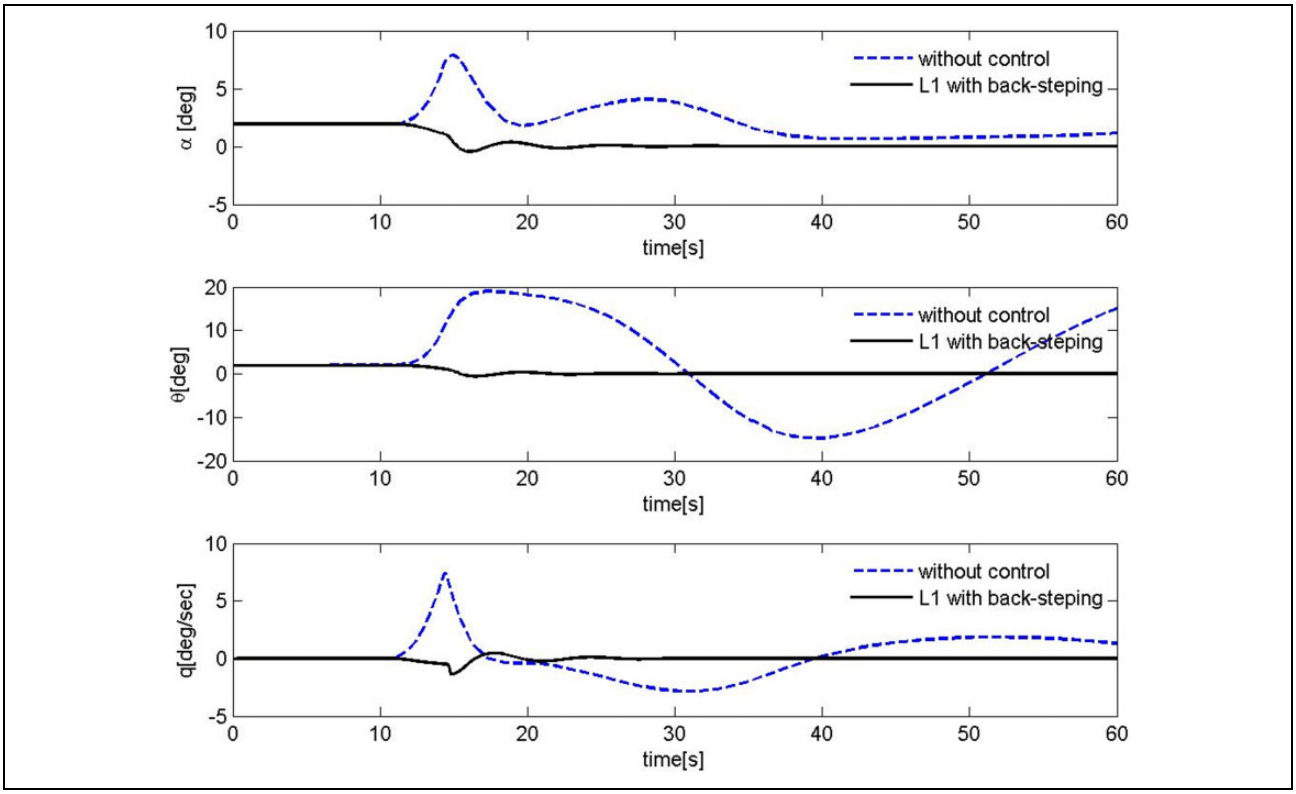

Figure 4. Attitude angles response.

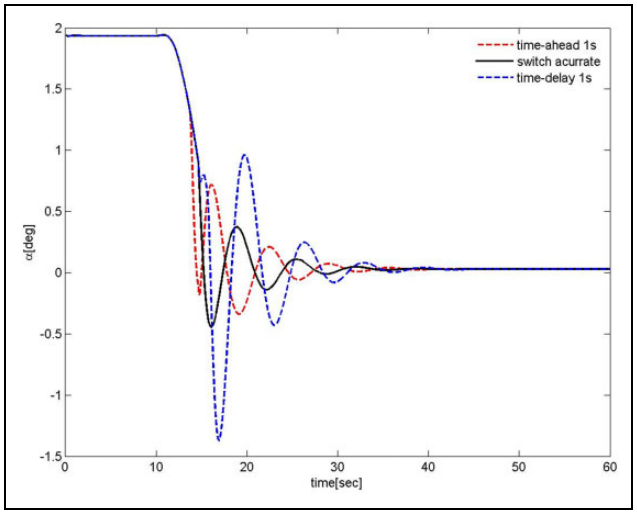

Figure 5. Attack angle dynamic response.

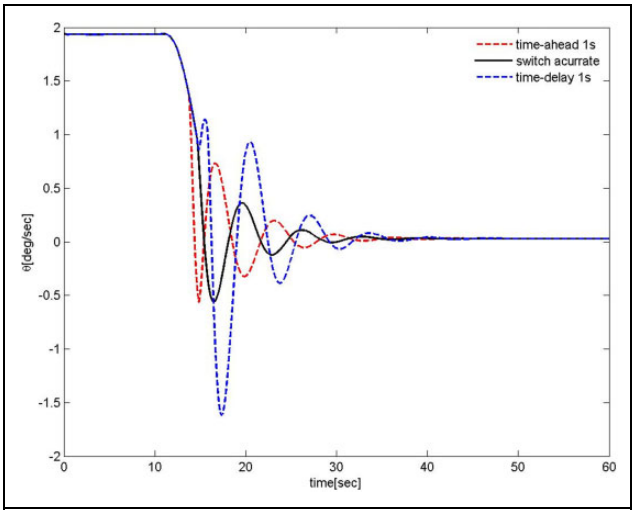

Figure 7. Pitch angle dynamic response.

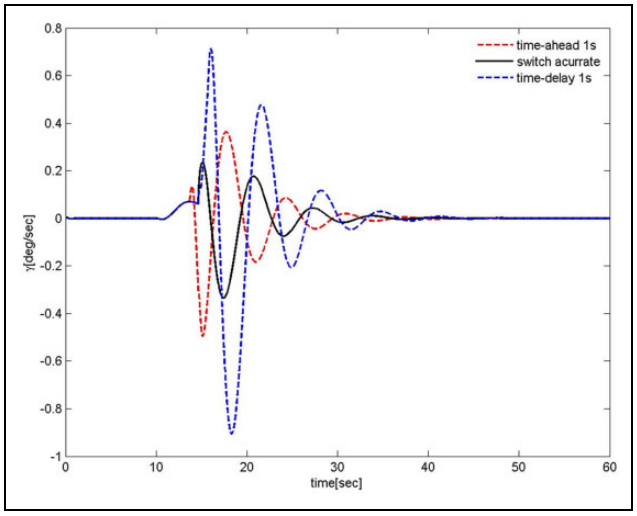

Figure 6. Track angle dynamic response.

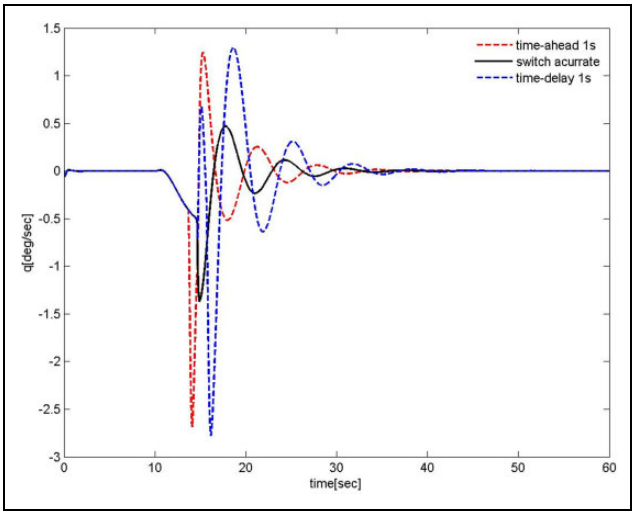

Figure 8. Pitch rate dynamic response.

Similar to proof 1, there is

$$\dot{L}_V = e_V \dot{e}_V = -k_V e_V^2 \tag{46}$$

where the design parameter is

$$k_V > 0 \tag{47}$$

For the Lyapunov function is negative, the velocity subsystem is stable.

Simulation verification and analysis

Using Matlab to calculate the balance state of different heights and velocities, this article simulates the situation of airdrop as shown in Table 6.

The initial state before the airdrop is $V = 221$ ft $\cdot$ s^{-1}, $\alpha = 1.9376°$, $q = 0°/\text{s}$, $\theta = 1.9376°$, and $H = 16.404$ ft. In the first 10 s, the plane is in the level situation, and at 10 s the goods start to move backward and are ready to leave the plane.

The L_1 adaptive backstepping controller for large transport aircraft airdrop heavy load is designed for the instability of the aircraft caused by the drop process. The controller parameters in the attitude subsystem are $k_1 = 1.2$ and $k_2 = 4$ with the static gains of $K = -20$, $\Gamma = 1000$, and $Q = 1$, and the low-pass filter is $C(s) = \frac{500}{s+500}$. The controller parameter of velocity subsystem is $k_V = 1.2$. The parameters of the PID control system are $k_P = 0.8$, $k_I = 0.1$, and $k_D = 0.04$.

Figure 3 is the chart for comparing the plane altitude and the velocity response with no controller or the L_1 adaptive backstepping controller. Figure 4 shows the dynamic response of flight angle, pitch angle, and pitch angle velocity in the two cases. From the comparison in Figures 3 and 4, we can see that the flight altitude, velocity, and attitude angles can be kept stable during the airdrop using this control

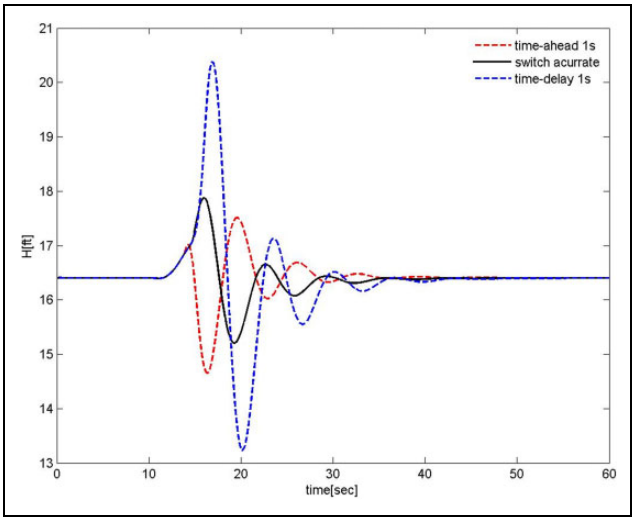

Figure 9. Height dynamic response.

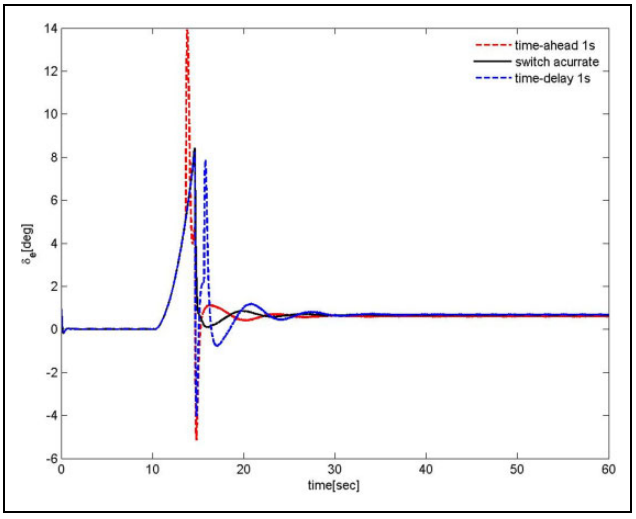

Figure 10. Elevator response.

method. If there is no proper control, the flight will change seriously, which will threaten the aircraft safety especially at the moment of cargos leaving the aircraft.

At the moment of airdrop, it is necessary to switch the control strategy for the model mutation and the switch moment is also very important for the flight's robust performance.

Figures 5 to 9 show the control effect in the three cases: accurate switch, time delay of 1 s and 1 s ahead of switch time. It can be seen that the control strategy in this article obviously has the control performance with short overshoot, short response time, and short adjustment time, showing the good stability and dynamic performance. At last the rapidity of the control method is shown in Figure 10 in the certain control and environmental cases. From the simulation results, we can see that the controller based on the L_1 adaptive backstepping can guarantee the flight performance and high robustness.

Conclusion

In this article, aimed at the airdrop, the backstepping is used for the velocity controller and the L_1 adaptive control combined with backstepping is proposed for the attitude control law. In view of the uncertainty existing in the system, the L_1 adaptive controller is used to estimate, compensate, and improve the control performance of the pure backstepping controller. By constructing the Lyapunov function, the system stability is proven. Simulation results show the effectiveness of the controller.

Acknowledgement

The authors would like to thank the anonymous reviewers for their helpful comments and valuable suggestions which improved this paper substantially.

Declaration of conflicting interests

The author(s) declared no potential conflicts of interest with respect to the research, authorship, and/or publication of this article.

Funding

The author(s) disclosed receipt of the following financial support for the research, authorship, and/or publication of this article: This study has been funded by the Shaanxi Industrial Science and Technology Key Project (grant no 2016GY-070) and Shaanxi Province Department of Education Key Project (grant no 2016JS017).

References

1. Xu B and Chen J. Review of modeling and control during transport airdrop process. *Int J Adv Robot Syst* 2016; 13(6): 1–8. DOI: 10.1177/1729881416678142.
2. Zhang HN, Zhang PT, and Cheng WH. Research of two different modeling methods of airdrop. *Sci Technol Eng* 2012; 12(6): 3896–3900.
3. Calise AJ and Preston D. Swarming/flocking and collision avoidance for mass airdrop of autonomous guided parafoils. *J Guid Control Dyn* 2008; 31(4): 1123–1132.
4. Bury Y, Morton SA, and Charles R. *Experimental investigation of the flow field in the close wake of a simplified C-130 shape: a model approach of airflow influence on airdrop.* In: *AIAA applied aerodynamics conference*, Honolulu, Hawaii, USA, 18–21 August 2008.
5. Raissi K, Mani M, Sabzehparvar M, et al. A single heavy load airdrop and its effect on a reversible flight control system. *Aircraft Eng Aeros Technol* 2008; 80(4): 400–407.
6. Chen J and Shi ZK. Aircraft modeling and simulation with cargo moving inside. *Chin J Aeronaut* 2009; 22(2): 191–197.
7. Cuthbert PA and Desabrais KJ. Validation of a cargo airdrop software simulator. In: *AIAA 17th aerodynamic decelerator systems technology conference*, Monterey, CA, 19 May 2003, pp. 1–11.
8. Jann T. *Coupled simulation of cargo airdrop from a generic military transport aircraft*. In: *AIAA 49th aerospace sciences*

meeting including the new horizons forum and aerospace expositon, Oriando, FL, 3–7 January 2011, pp. 2011–2566.
9. Chen M, Tao G and Jiang B. Dynamic surface control using neural networks for a class of uncertain nonlinear systems with input saturation. *IEEE Trans Neural Netwk Learn Syst* 2015; 26(9): 962–967.
10. Liu R, Sun X, and Dong W. Dynamics modeling and control of a transport aircraft for ultra-low altitude airdrop. *Chin J Aeronaut* 2015; 28(2): 478–487.
11. Xia YZ, Shi ZK, and Xu B. Back-stepping control design for transport aircraft in airdropping heavy cargo. In: *The 34th Chinese control conference*, Vol. 22(2), Hangzhou Dianzi Univ, 28–30 July 2015, pp. 5718–5723.
12. Zhang J, Xu H, Zhang D, et al. Safety modeling and simulation of multi-factor coupling heavy-equipment airdrop. *Chin J Aeronaut* 2014; 27(5): 1062–1069.
13. Chen M and Ge SS. Adaptive neural output feedback control of uncertain nonlinear systems with unknown hysteresis using disturbance observer. *IEEE Trans Industr Elect* 2015; 2015: 962–967.
14. Xu GZ and Sun XX. Heavyweight airdrop pitch flight control law design based on feedback linearization theory and variable structure control. In: *AIAA Guidance, navigation and control conference (CGNCC), 2014 IEEE Chinese*. 13–17 January 2014, pp. 962–967. IEEE.
15. Zhang HY and Shi ZK. Variable structure control of catastrophic course in airdropping heavy cargo. *Chin J Aeronaut* 2009; 22(5): 520–527.
16. Ward M and Costello M. Adaptive glide slope control for parafoil and payload aircraft. *J Guid Control Dyn* 2013; 36(4): 1019–1034.
17. Zhang C, Peng C, Liu J, et al. Flight control verification and clearance for a transport aircraft using stochastic robust analysis and synthesis. In: *AIAA Guidance, navigation and control conference (CGNCC)*, *IEEE Chinese*, 13–17 January 2014, pp. 2763–2767. IEEE.
18. Xu B and Zhang P. Composite learning sliding mode control of flexible-link manipulator. *Complexity* 2017; 2017: 6. DOI: 10.1155/2017/9430259.
19. Xu B and Zhang P. Minimal-learning-parameter technique based adaptive neural sliding mode control of MEMS gyroscope. *Complexity* 2017; 2017: 8. DOI: 10.1155/2017/6019175.
20. Raptis IA, Valavanis KP, and Moreno WA. System identification and discrete nonlinear control of miniature helicopters using back stepping. *J Int Robot Syst* 2009; 55(2–3): 223–243.
21. Li C, Zhang Y, and Li P. Full control of a quadrotor using parameter scheduled back stepping method: implementation and experimental tests. *Nonli Dyn* 2017; 89(2): 1259–1278.
22. Li C, Zhang Y, and Li P. Extreme learning machine based actuator fault detection of a quadrotor helicopter. *Adv Mech Eng* 2017; 9(6): 1–10.
23. Xu B. Disturbance observer based dynamic surface control of transport aircraft with continuous heavy cargo airdrop. *IEEE Trans Syst Man Cybern Syst* 2017; 47(1): 161–170.
24. Cao CY and Hovakimyan N. Design and analysis of a novel L1 adaptive controller, part I: control signal and asymptotic stability. In: *American control conference*, Minnesota, USA, 14–16 June 2006, pp. 3397–3402.
25. Cao CY and Hovakimyan N. Design and analysis of a novel L1 adaptive controller, Part II: Guaranteed transient performance. In: *American control conference*, Minnesota, USA, 14–16 June 2006, pp. 3403–3408.
26. Christopher MC, Cao CY, and Hovakimyan N. Simulator testing of longitudinal flying qualities with L1 adaptive control. In: *AIAA Atmospheric flight mechanics conference*, Hawaii, 18–21 August 2008, pp. 1–14.
27. Patel VV, Cao CY, Hovakimyan N, et al. L1 adaptive controller for tailless unstable aircraft. In: *American control conference*, New York, 9–17 July 2007, pp. 5272–5277.
28. Cao CY and Hovakimyan N. Design and analysis of a novel L1 adaptive control architecture with guaranteed transient performance. *IEEE Trans Autom Control* 2008; 53(2): 586–591.
29. Hovakimyan N and Cao CY. State feedback in the presence of matched uncertainties. *L1 Adaptive control theory: Guaranteed robustness with fast adaptation*. Philadelphia, PA: Society for Industrial and Applied Mathematics 2010, pp. 17–20.